

Original Article

Sustainable Innovation in the Design of $f'c=210$ kg/cm² Concrete Reinforced with Aguaje Shell Fibre and Prawn Exoskeleton Ash: Mechanical Properties and Durability

Aylthon Gustavo Poma Contreras^{1*}, Kenny Yoseef Pizarro Avellaneda¹, Anthony Jesus Barahona Maximiliano¹, Manuel Ismael Laurencio Luna¹

¹Faculty of Civil Engineering, Continental University, Huancayo, Perú.

*Corresponding Author : 72508315@continental.edu.pe

Received: 05 December 2025

Revised: 04 January 2026

Accepted: 03 February 2026

Published: 23 March 2026

Abstract - The construction industry has a high environmental impact due to the intensive use of cement in concrete production, which leads to significant carbon dioxide (CO₂) emissions. In Peru, considerable quantities of agro-industrial and aquaculture by-products, especially waste from aguaje (*Mauritia flexuosa*) and shrimp exoskeletons, are typically generated and not recycled, leading to various environmental complications. In this context, this study evaluates the use of these wastes as alternative materials in the production of concrete with a characteristic compressive strength of $f'c = 210$ kg/cm². Aguaje Shell Fibre (ASF) was incorporated at proportions ranging from 0.00% to 1.70% by volume, while Shrimp Exoskeleton Ash (PEA) was added at contents between 0.00% and 2.50% by weight of cement. The behaviour of fresh concrete was evaluated through slump, temperature, unit weight, air content, and bleeding tests. In the hardened state, compressive strength, indirect tensile strength, flexural strength, and resistance to sulphate attack were determined at curing ages of 7, 14, 28, and 50 days. The results show that the combined incorporation of ASF and PEA reduces bleeding and slightly decreases workability, while remaining within acceptable ranges for structural applications. Mechanical properties improved progressively until an optimum dosage of 1.30% ASF and 1.50% PEA was reached. At this level, compressive strength increased by approximately 31.24%, indirect tensile strength by 77.60% and flexural strength by 93.89% at 28 days compared to the reference concrete. In addition, an improvement in resistance to sulphate attack was observed. Higher dosages resulted in reduced performance due to fibre agglomeration and loss of continuity in the cement matrix. Overall, the results indicate that the combined use of aguaje shell fibre and shrimp exoskeleton ash is a viable option for producing more sustainable concrete with improved mechanical properties and durability, while promoting waste valorisation and reducing the use of conventional materials.

Keywords - Shrimp Exoskeleton Ash, Aguaje Shell Fibre, Concrete.

1. Introduction

The construction sector significantly contributes to the world's energy consumption. It contributes to around 40% of primary energy consumption, 33% of CO₂ emissions, and 60% of the earth's lithosphere raw materials consumption [1]. One of the most essential materials in the construction of a building is concrete, which is made of water, coarse and fine aggregates, and, most importantly, cement. Cement is a critical component due to its adverse effect on the environment [2]. The process of manufacturing cement involves the most energy-demanding and greenhouse gas emissions contributing process: clinker calcination. If nothing is done to alleviate the situation, cement manufacturing will be responsible for approximately 23% of global CO₂ emissions by 2050 [3]. In the Peruvian context, concrete output surged precipitously to 671,000 m³ by May 2024 [4, 5], catalysed by proliferative infrastructural megaprojects

encompassing domiciles, viaducts, arterials, aerodromes, and mercantile complexes [6]. This acceleration precipitates profound sustainability dilemmas, as concrete's genesis is inextricably tethered to cement's industrial elaboration.

Technically and ecologically, the use of agro-industrial and aquaculture waste as alternative materials in the cementitious matrices is viable. Peru has made big gains in the aquaculture sector, particularly in the cultivation of shrimp harvesting, with shrimp harvests of 39,348 metric tonnes in 2023 [7]. This record harvest created plenty of chitinous cuticles, the large majority of which are discarded, making the situation of biosphere pollution worse. This buildup of organic waste not only creates the problem of macro and micro ecologies, but it also creates a problem for people and public health due to the presence of pathogens, bad smells, and the presence of rats [8]. Similarly, in the Peruvian jungle,



particularly in the department of San Martín, as shown in Figure 1, aguaje production generates a high volume of waste, since after the pulp is extracted for commercialisation, the shells and seeds are discarded without effective use. It is estimated that approximately 50 tonnes of waste are generated daily, which exacerbates the pollution problem and represents a missed opportunity for the reuse of resources with high potential [9-11].

Numerous studies have demonstrated that the incorporation of organic residues can enhance specific properties of concrete. *Cocos nucifera* fibre has demonstrated amplification of compressive indices [12]; *Saccharum officinarum* bagasse ash has curtailed fissurative micropropagation, enhancing resilience [13]; likewise, cocoa husk fibre increases the workability of concrete [14]. On the other hand, in the aquaculture sector, crab and oyster shells have been used to improve the tensile, flexural, and compressive strength of concrete [15-17]. However, most of these studies have focused on the incorporation of a single type of residue, without jointly analysing the interaction between plant-based fibres and marine-derived ashes within the same cementitious matrix. As a result, there is a lack of comprehensive understanding of how combined organic additions may interact and influence concrete performance.

Here, one can notice the lack of understanding of the mechanical behaviour, durability, and workability of hybrid concrete consisting of Aguaje Shell Fibre (ASF) and Shrimp Exoskeleton Ash (PEA). This establishes the scope of use of these materials for structural and semi-structural applications. The use of these two by-products is aimed at determining the possible combined effects of the fibre reinforcement and the filling and nucleation effects of ash on concrete, and is expected to sustain concrete performance and reduce the use of conventional cement materials.

The main objective of this research is to experimentally evaluate a biohybrid concrete that integrates ASF and PEA simultaneously as sustainable materials within a conventional cementitious matrix. The study is carried out through laboratory-based experimental testing, considering different incorporation levels of both residues, and focuses on the assessment of the concrete's fresh, mechanical, and durability-related properties.

For this purpose, a characteristic compressive strength of $f_c = 210 \text{ kg/cm}^2$ is adopted, as this strength level is widely used in low- to mid-rise buildings, pavements, and basic structural components in developing countries. This allows for a practical evaluation of the feasibility of biohybrid concrete in real-world construction applications.

Accordingly, this research addresses the following research questions:

- What ramifications does the dual integration of ASF and

PEA bear upon the plastic, mechanical, and durability spectra of concrete formulated at $f_c = 210 \text{ kg/cm}^2$?

- Does a specific admixtural synergy elicit optimization in mechanical fortitude, sulphate inertness, and workability?

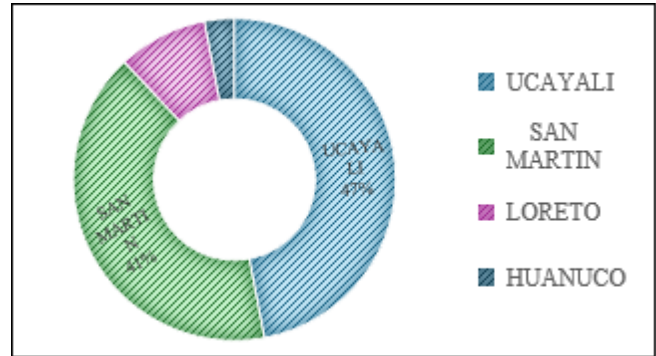


Fig. 1 Departments with the highest aguaje production in Peru

2. Literature Review

Because there is still very limited civil engineering research on the use of aguaje shell fibres and shrimp exoskeletons in concrete, it becomes necessary to first explore their characteristics and behaviour in other application fields. In addition, previous studies involving different plant fibres and animal-based ashes will be reviewed to provide context and help anticipate their potential influence on the mechanical performance and durability of concrete.

Mauritia flexuosa, commonly known as “aguaje,” is a palm species of great ecological importance native to the Peruvian Amazon. This species supports a wide range of industrial and productive activities [18]. The pulp from the fruit of this plant is also used in the manufacture of flour, which is used in baked goods and the preparation of high-energy foods, and is widely eaten as a juice, ice cream, and sweet-based products. Its fruit is also rich in carotenoids, especially β -carotene. [19, 20]. After its seeds and pulp, which have cosmetic and dermatological value and are used as moisturizers, and its regenerative oil, which is extracted and used in the cosmetic and dermatological industries, are highly valued [21].

Members of the *Litopenaeus vannamei* and *Penaeus monodon* taxa exemplify the backbone of penaeid aquaculture and are the crustaceans commonly called the white and black tiger shrimps. These decapods are of worldwide commercial fishing importance and significantly contribute to the fishing economy of the Austro-Asian region [22]. With the chitinous skeleton of decapods made up of aminopolysaccharides, their biotransformation processes yield chitosan, a polysaccharide of bioactive functional potential, i.e., antimicrobial, antioxidant, etc.

Chitosan is valuable in many sectors. In the food industry, it is an antimicrobial food preservative [23], and in

biopharmacology, it is used in drug delivery systems and bioresorbable sutures [24]. In agriculture, it is used as a biostimulant and fungicidal [25]; and in the cosmetics industry, its skin bioremosive properties are used [26].

In the Malaysian jurisdiction, the assimilation of unprocessed Agave filaments into concreterary matrices was appraised by the edificatory bureau. Utilizing fibrous dosages (0% to 0.75%) of 19 mm elongation, they discerned that a 0.45% admixture optimized compactivity, surpassing the 3 MPa compressive strength, compared to the standard of 2 MPa.

In flexural strength, after 56 days, it exceeded 0.6 MPa, while the standard was less than 0.5 MPa [27]. A counterpart inquiry from Ecuador's geoengineering faculty dissected *Cocos nucifera* fibre integration (4 cm, 0.5% and 1%). After 56 days, a 0.5% dose escalated resistance from 26.91 to 34.15 MPa, while 1% incorporation curtailed CO₂ emissions by 5% [28].

In the Indian subcontinent, analyses of *Coryota urens* lignofibres (1–5%) denoted 3% as optimal, achieving 55.4 MPa compressive strength. At said infill, axial rupture increased from 4.3 to 4.6 MPa, and flexural tenacity from 4.83 to 5.36 MPa [29]. Additionally, ovine keratinous threads (2–3%) augmented axial and bending resilience by 32.7% and 20.8%, respectively [30]. *Corchorus capsularis* inclusions (1.5%) exhibited a 19.7% compressive and 30.8% tensile augmentation, albeit with rheological detriment [31].

The Abyssinian civil corpus scrutinized pyroprocessed *Oryza sativa* husk particulates as cementitious surrogates. Ash incorporation (10–20%) refined rheology and chrono-setting behavior via granulometric superiority, while fortifying compressive, tensile, and flexural capacity alongside hydroresistance and ion-intrusion antagonism [32–34].

In the Pakistani context, *Zea mays* cob calx was explored for eco-constructive substitutions. While minimal incorporations (5–10%) proved inert in performance modulation, a 30% substitution culminated in elevatory effects, compressive strength rose by 11.62%, and tensile resilience by 10.56% [35, 36].

A profusion of investigational enterprises in the Lusophone territories of South America, particularly within Brazilian precincts, has explored the assimilation of phytogetic detritus as fractional surrogates for cementitious matter in ecoconcrete formulations. Amid escalating imperatives to diminish the anthropogenic carbon miasma, the Secretariat of Scientific and Technological Affairs probed the incorporation of *Musa foliar* calx (BLA). With incrementations of 0%, 5%, 10%, and 15% BLA, augmentative tendencies in mechanical comportment were catalogued, and an 18% accretion in compressive modulus at a curing epoch of 90 days was chronicled [37].

Concomitantly, the Facultative Conglomeration of Civil Artifice and Architectonic Engineering investigated the influence of *Gossypium* stalk calcinate in aeriform, autonomously consolidating concrete. Using proportions of 5%, 10%, and 20%, they reported an uptick in compressive potential to 33 N/mm² vis-à-vis 29 N/mm² for unamended specimens, post 28-day hydration. Tensile fortitude rose from 2.8 N/mm² to 3.3 N/mm², while flexural metrics increased from 5.4 N/mm² to 6.6 N/mm² [38].

Parallel inquiries at the Technological Faculty's Civil Division examined pozzolanic categorization of *Bambusa foliar* ash. Specimens incorporating 5% and 10% of this calcined foliar matter attained a mean compressive threshold of 33.5 MPa at 28 days. Further evolution at 56 days denoted incremental rises of 1.84% and 0.12% for 5% and 10% dosages, respectively. Ancillary benefits included diminution in aqueous sorptivity and augmented sulphatic resilience. The prescriptive consensus discouraged surpassing 10% substitution for optimal performance [39, 40].

A deficiency of naturally occurring lithoidal aggregates prompted the Filipino Faculty of Agro-Engineering and Technological Inquiry to explore the substitutive use of *Callinectes sapidus* exoskeletal ash (10% and 15%) as an arenaceous substitute. However, there were clearly negative results: compressive metrics lessened by 46.26% and flexural indices dropped by 50.82%. Nevertheless, it was suggested that flexible reutilization with a non-load-bearing structure be explored [41].

In contrast, the Department of Civil Engineering reported positive results from uncalcined *C. sapidus* integument inclusion as a fine granular component. They tested 5%, 7%, and 8% inclusion and reported the most notable mechanical improvement at the 7% level [42].

In the Niger-Congolese bioregion, *Senilia senilis* conchiform remnants were used as macro-aggregates. The control compressive strength recorded was 25.71 N/mm², while the 10% conchaceous infusion was reduced to 23.23 N/mm². The tensile strength also reduced from 2.55 N/mm² to 2.24 N/mm² [43]. Partial admixture of lithic particulates and *Tympanotonos fuscatus* exuviae calx (5%–100%) also yielded compressive retrogression from 22.9 N/mm² to 13.8 N/mm² under total substitution [44]. Due to the negative results, a reconditioning of materials and dosages is required to mitigate structural deficiencies.

On the other hand, Malaysian geotechnical scholars celebrate the positive outcome of using the partial cementitious replacement with marine calcareous ash in lightweight cementitious composites. Using an admixture proportion of 5% to 30%, concrete with 15% seashell ash showed an increase of 12.41%, 17.95% and 15.89% in compressive, flexural, and tensile strengths, respectively,

demonstrating the potential of molluscan detritus as an alternative functional filler [45].

From the existing literature, it is clear that most inquiries have concentrated on mono admixture schemes of organic fibre or bio-calcinate as individual concrete modifiers, documenting incremental progress in particular confined parameters. Still, a noticeable gap exists in the more comprehensive studies at an architectural-grade strength ($f'c=210 \text{ kg/cm}^2$) on the combined effect of various biogenic types in a single cementitious system.

Thus, the ASF-PEA dual bioformulation model proposed here seeks to enable a more granular understanding of the rheological, mechanostructural, and resistance to different temporal degradation of composite material, and as such situates the clear context of composite material relative to the most recent existing empirical body of evidence.

3. Materials and Methods

3.1. Cement

Cement is a powdery adhesive substance that, when combined with water, creates a bindable paste that can set and bind itself with other materials. Once solidified, the paste adds strength and cohesion to the composite material [46]. For this research, Type I Portland cement was examined. The table below (Table 1) describes the physicochemical properties of fineness, specific gravity, and chemical composition [calcium oxide (CaO), silicon dioxide (SiO₂), aluminum oxide (Al₂O₃), and iron oxide (Fe₂O₃)] that were used in the study. The cement's bonding chemical and mechanical properties result from the combination of the given oxides.

Table 1. Physical and chemical properties of cement

Physical Characteristics	Chemical Characteristics
Colour: Light grey	Calcium oxide (CaO): 60-67%
Fineness (m ² /kg): 225 - 400 (Blaine)	Silicon dioxide (SiO ₂): 17-25%
Density (g/cm ³): 3.10 - 3.15	Aluminium oxide (Al ₂ O ₃): 3-8%
Specific weight: 1.2 - 1.4 g/cm ³ (suelto)	Iron oxide (Fe ₂ O ₃): 0.5-6%
Normal consistency (%): 26 - 33	Sulphur trioxide (SO ₃): ≤ 3.5%
Initial setting time: 45 - 60 min	Magnesium oxide (MgO): ≤ 5%
Final setting time: 6 - 10 h	Loss on ignition: ≤ 4%

3.2. Coarse Aggregate

Coarse aggregate consists of rock or gravel particles greater than 4.75 mm and is vital to ensuring that concrete maintains its durability and structural performance by providing strength, stability, and volume [47, 48]. For this

research, coarse aggregate from the Pilcomayo quarry in Huancayo was employed, as shown in Figure 2. The particle size distribution given in Table 2 indicates that the retained materials for 89.30% of the samples span from 9.50 mm (3/8 inch) to 4.75 mm (No. 4). This size distribution, having a larger proportion of smaller coarse particles, is ideal for the purposes and scope of this study.

Table 2. Particle size distribution

Sieve	Opening	% Retained	% Accumulated Retained	% Passing
1"	25.00	0.00	0.00	100.00
3/4"	19.00	0.00	0.00	100.00
1/2"	12.50	3.30	3.30	96.70
3/8"	9.50	34.20	37.50	62.50
N°4	4.75	55.10	92.60	7.40
N°8	2.36	5.50	98.10	1.90
Bottom		1.90	100.00	0.00



Fig. 2 Coarse aggregate

3.3. Fine Aggregate

Fine aggregates are a granular material, usually sand, that passes through the 4.75 mm (No. 4). They contribute strength, stability, and volume to concrete, thus enhancing its durability and structural capacity [48]. During this investigatory endeavor, we collected particulates of different granulations from the Pilcomayo extraction locus in Huancayo (Figure 3).

The granule dispersion, shown in Table 3, indicates that 95.90% of the material passes through sieve No. 100 (0.15 mm), while only 2.50% is retained on sieve No. 4 (4.75 mm). Such a construction of particulates suggests a profile of good gradation, which can contribute to an increase in cohesion and a better, denser, concrete matrix.

Table 3. Granulometry

Sieve	Opening	% Retained	% Accumulated Retained	% Passing
3/4"	19.00	0.00	0.00	100.00
1/2"	12.50	0.00	0.00	100.00
3/8"	9.50	0.00	0.00	100.00
N°4	4.75	2.50	2.50	97.50
N°8	2.36	13.40	15.90	84.10
N°16	1.18	17.80	33.70	66.30
N°30	0.60	20.10	53.80	46.20
N°50	0.30	24.80	78.60	21.40
N°100	0.15	17.30	95.90	4.10
Bottom		4.10	100.00	0.00

3.4. Aguaje Shell Fiber (ASF)

The palmoid plant *Mauritia flexuosa*, locally called the “burití,” is an important ethnobotanical resource in the Amazonian geocultural region of Peru. It has an edible, carotenoid-rich, orange drupe that is used in a number of food products, including sorbets, infusions, and other foods. The fruit’s biochemical arsenal, prominently β -carotene (a provitamin A), is important for the maintenance of good health, particularly for the eyes and skin. The aguaje also has significant socio-cultural value for its alleged therapeutic (particularly as an antioxidant) and folkloric properties for hair, as well as for eco-entrepreneurship in the rainforest. [49].

The filament of aguaje shells has a tensile tenacity of 585 ± 178 MPa and a bulk density ranging between 0.63 and 1.12 g/cm³, as shown in Table 4. The volumetric percentage of the

moisture content is between 7.7% and 9.1%, positioning him in the hygroscopic zone of the moisture balance. The above physico-mechanical parameters indicate that aguaje shells can be microreinforcements in composites, and as such, they are likely to improve the structures ecologically and physically.

Table 4. Physical and mechanical properties of aguaje shell fiber [50]

Physical and Mechanical Properties	
Physical properties	Value
Apparent density	0.63-1.12 g/cm ³
Moisture content	7.7-9.1%
Mechanical properties	Value
Tensile strength	585 ± 178 MPa
Elongation at break	40.6-27.6%
Modulus of elasticity	9.53 ± 2.8 GPa

In Figure 3, the first stage of aguaje shell fibre production encompasses the collection of the fruit (Figure 3(a)). The shells must be separated and then subjected to the washing and drying process for 48 hours in order to remove moisture and surface impurities (Figure 3(b)). After drying, the fibres are ready for use (Figure 3(c)). Processed fibres are of irregular shape, having lengths that are roughly 10 to 30 mm and with diameters of 1 to 3 mm, giving them an aspect ratio (L/D) of about 5 to 15. These measurements were taken through visual inspection of the fibres in Figure 3(c). No chemical surface treatments were done. Fibres were not pre-mixed with the other components of the concrete. During the concrete preparation, the fibres were added to the dry mix in order to achieve an even dispersion and to minimize fibre clumping. The fibres were added in the following volume fractions: 0.00%, 0.70%, 0.90%, 1.10%, 1.30%, 1.50%, and 1.70%. [28].



Fig. 3 Aguaje shell fiber

3.5. Shrimp Exoskeleton Ash (PEA)

Carapacial residues of decapod crustaceans, incidentally procured via bycatch, are constituted primarily of chitinous polysaccharides and calcareous particulates, both exploitable across multifarious industrial domains [51]. Illustratively, within agronomical praxis, such exuviae may be comminuted and amalgamated into fertilising substrates to augment their

physicochemical framework and furnish edaphic nourishment [25]. Chitosan, derived from shrimp exoskeletons, has been used in the adsorption and removal of a variety of pollutants in the field of wastewater treatment [52]. In addition to this, shell residues from shrimp have been used in the formulation of cosmetics and in medical and surgical dressings, due to their antibacterial properties and the ability to retain moisture

[26, 24]. This form of reuse is environmentally sustainable as it enhances the value of seafood waste, diminishes its environmental burden, and promotes the use of fully biodegradable materials. As shown in Table 5, shrimp exoskeletons also have a considerable value in the construction field. The compressive strength values of shrimp exoskeletons range from 80 to 120 MPa, while their tensile strength is in the range of 70 to 100 MPa, which shows that they have considerable construction value as they can be used to make construction materials that can withstand considerable pressure.

Table 5. Physical, chemical, and mechanical properties of shrimp exoskeleton ash [53]

Physical properties	
Property	Value
Specific weight	1.5 g/cm ³
Thermal conductivity	0.1-0.3 W/m.k
Mechanical properties	
Hardness	40-70 MPa
Elasticity	1-3 GPa
Compressive strength	80 a 120 MPa
Tensile strength	70 a 100 MPa
Impact resistance	50 J/m ²
Stiffness	1-3 GPa
Chemical properties	
Calcium carbonate (CaCO ₃)	20:30%
Magnesium oxide (MgO)	1-5%
Silicon oxide (SiO ₂)	0.5-3%
Aluminum oxide (Al ₂ O ₃)	0.5-2%
Iron oxide (Fe ₂ O ₃)	0.1-1%

Approximately 20-30 % of shrimp skeletons (exoskeletons) contain bound calcium carbonate (CaCO₃) that is of Industrial interest for use in cement-based materials. Under normal conditions (without major alterations), calcium carbonate in cement is the result of the carbonation process of calcium hydroxide (Ca (OH)₂), which has occurred as a result of the reaction of cement with atmospheric CO₂. In the current scenario, however, CaCO₃ is already in the skeleton structure. This means the use of shrimp exoskeletons in cement provides a naturally occurring, chemically active, and bound mineral additive directly to the cementitious matrix. Scanning Electron Microscopy (SEM) reveals the presence of calcite and aragonite morphologies of calcium carbonate crystals, forming on the binder surface; these act as heterogeneous nucleation sites (Figure 4). The presence of these carbonate crystals is likely to enhance the binder matrix densification, reduce capillary porosity, and improve the mechanical strength and durability of the concrete [54, 55]. Therefore, the proposed use of shrimp exoskeletons in concrete gives evidence for the sustainable reuse of an available marine waste

and, at the same time, improves the cementitious composite’s physico-mechanical properties, aiding the economical manufacture of high-quality concrete materials.

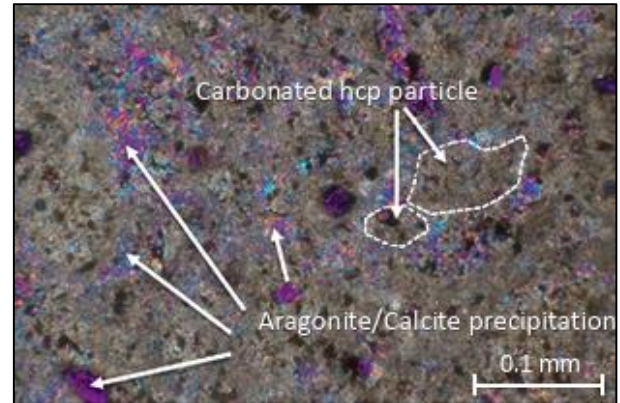


Fig. 4 Scanning Electron Microscopy analysis of calcium carbonate [54]

The ash derived from shrimp exoskeletons represents the final stage of the process illustrated in Figure 5. The exoskeletons were first washed and air-dried, followed by oven drying at temperatures between 60 and 80 °C to eliminate residual moisture. They were then calcined at temperatures ranging from 600 to 800 °C in order to decompose the organic matter and convert the material into a brittle solid. This calcined material was subsequently ground in a mortar and sieved through a 200 µm mesh to obtain a fine, homogeneous ash. The resulting ash was incorporated into the mixtures at replacement levels of 0%, 1.50%, 2.00%, and 2.50% [56].



Fig. 5 Shrimp exoskeleton ash

Table 6 presents the concrete mix design developed to achieve a target compressive strength of $f'c=210$ kg/cm². The proportions of cement, fine aggregate, coarse aggregate, and water were kept constant in all mixtures. Within this fixed base composition, Aguaje Shell Fibre (ASF) and Shrimp Exoskeleton Ash (PEA) were added in varying amounts. ASF contents ranged from 2.75 kg/m³ to 6.68 kg/m³, while PEA

contents varied between 5.90 kg/m³ and 9.83 kg/m³. For identification purposes, the different mixtures were labeled M1 to M7, corresponding to the following incorporation

levels: ASF at 0.00%, 0.70%, 0.90%, 1.10%, 1.30%, 1.50%, and 1.70%, and PEA at 0.00%, 1.50%, 2.00%, 2.50%, 1.50%, 2.00%, and 2.50%, respectively.

Table 6. Mix design for f'c=210 kg/cm2

Samples	Nomenclature	Cement (Kg)	Fine aggregate (Kg)	Coarse aggregate (Kg)	Water (l)	ASF	PEA
0.00%(ASF)+0.00%(PEA)	M1	393.00	813.00	899.00	220.00	0.00	0.00
0.70%(ASF)+1.50%(PEA)	M2	393.00	813.00	899.00	220.00	2.75	5.90
0.90%(ASF)+2.00%(PEA)	M3	393.00	813.00	899.00	220.00	3.54	7.86
1.10%(ASF)+2.50%(PEA)	M4	393.00	813.00	899.00	220.00	4.32	9.83
1.30%(ASF)+1.50%(PEA)	M5	393.00	813.00	899.00	220.00	5.11	5.90
1.50%(ASF)+2.00%(PEA)	M6	393.00	813.00	899.00	220.00	5.90	7.86
1.70%(ASF)+2.50%(PEA)	M7	393.00	813.00	899.00	220.00	6.68	9.83

Once all the materials and their respective dosages had been obtained, the concrete was prepared. The cement acted as a binding agent, binding the other components together, while the coarse and fine aggregates provided strength and structural stability. The water, for its part, facilitated the hydration and setting of the cement, forming the cement paste that gave the mixture its cohesion. Once a homogeneous mixture was obtained, tests were carried out on the fresh and hardened concrete to evaluate its properties and behavior.

3.6. Tests

For the battery of concrete blend evaluations delineated infra, Aguaje Shell Fibres (ASF) were incorporated at volumetric fractions of 0%, 0.7%, 0.9%, 1.1%, 1.3%, 1.5%, and 1.7%, while Shrimp Exoskeleton Ash (PEA) was intercalated at dosages of 0%, 1.5%, 2.0%, 2.5%, 1.5%, 2.0%, and 2.5%, as detailed in Table 6.

3.6.1. Fresh Concrete

Before placement and setting of fresh concrete, a slump test was conducted to assess its workability and fluidity according to MTC E 70. The test involves filling a frustoconical mold (30.5 cm height, 20.3 cm base diameter) in three equal layers. Each layer is compacted with 25 strokes of a 16 mm diameter and 600 mm long tamping rod. After leveling the last layer, the mold is removed vertically. The slump, which is the height of the vertical deformation of the concrete, is noted.

Temperature regulation of fresh concrete was done in accordance with MTC E 724. A concrete sample was placed in a thermally insulated container, and a calibrated bimetallic thermometer (with a measurement range of 0-50°C) was used to measure the temperature at a depth of 7.5 cm. Temperature was recorded after a period of 2 to 5 minutes of thermal stabilization.

In compliance with MTC E 713, bleeding tests were performed to evaluate the rise of water in the freshly made

concrete. Water was added to the mixture in a measuring cylindrical container of 14 liters (25cm diameter and 28cm height) to a level of 10 inches. The container was sealed to avoid water evaporation. Water that formed on the concrete surface was collected and measured in the first 10 minutes of the first four tests. Subsequent tests collected water every 30 minutes. The timing and volumes of water collected were recorded precisely to the milliliter.

The fresh concrete’s air content was measured in accordance with MTC E 706, using a Washington pressure meter. Concrete was poured in layers, and 25 blows were made for each layer. After sealing the chamber, water was added through the inlet until air was expelled through the outlet. Pressure was applied until the gauge needle was stable at zero, then the pressure was released, and the bottom valve was opened. After five tamping blows, the air content was recorded.

Finally, using the Washington container, the fresh concrete’s unit weight was established in accordance with MTC E 714. Concrete was uniformly distributed in three layers, with each layer being compacted to the rod (5/8-inch diameter and is 24 inches long) with 25 tamping blows and struck between 10 and 15 times with the mallet to ensure there were no voids. The surface was smoothed, and a calibrated scale was used to measure the weight of the container. The unit weight was calculated in kg/m³ by getting the net mass after subtracting the tare weight, and dividing this by the container’s volume.

3.6.2. Hardened Concrete

The mechanical behavior of the concrete was assessed by evaluating its compressive, tensile, and flexural strengths under varying loading conditions. To understand how the material behaves under axial loads, compressive strength tests were conducted. This test was performed according to MTC E 704, using 63 concrete cylindrical specimens, 4 inches in diameter and 8 inches in height. The specimens were wrapped

in plastic film to avoid moisture loss and were cured in an environmental chamber set at 20 ± 2 °C and $90 \pm 5\%$ RH for 7, 14, and 28 days. When the curing time was completed, the specimens were subjected to axial load compression using a compression testing machine. The load was applied at a controlled rate of 0.25 ± 0.05 MPa/s until failure.

As outlined in MTC E 708, the splitting tensile test was performed to find the indirect tensile strength of concrete. For this test, 63 cylindrical specimens were made with dimensions of 15 cm in diameter and 30 cm in height. The specimens were cured at 23 ± 1.7 °C and $50 \pm 5\%$ relative humidity in controlled environmental chambers for 7, 14, and 28 days. After the curing period, the tests were conducted using a Universal Testing Machine (UTM), where a controlled load was applied at a rate of 50 and 100 kN/min until the specimen failed. The failure load was then recorded.

The concrete beam samples were subjected to flexural strength tests to determine their maximum resistance to bending stresses. In accordance with MTC E 711 guidelines, 21 prismatic samples measuring 15 cm × 15 cm × 60 cm were prepared and cured for 28 days. After 28 days, these specimens were placed in the Universal Testing Machine (UTM), with a free span of 50 cm between the supports and the load applied at two points located at a third of the span, using a controlled loading rate to induce failure of the specimens at a bending stress of 0.9 to 1.2 MPa. The maximum load applied and the deflection at the centre of the span were recorded for all samples.

Finally, the sulfate attack resistance test evaluates the condition of concrete exposed to severe chemical aggression, typical of sulfate-congested soil or water, e.g., areas near coastal water, water treatment plants, chemical industry, mining, etc. Following E.060 standards, cylindrical test specimens measuring 15 cm in diameter and 30 cm in height were cured in a solution with a sulfate concentration of 50,000 ppm, classified as very severe exposure. Given the critical nature of this exposure, curing was applied for 50 days, which allowed the effects of sulfate attack to be analyzed in both standard concrete and concrete modified with aguaje shell fiber and shrimp exoskeleton ash.

4. Results

4.1. Fresh Concrete Characteristics

The ranges in Table 7 describe the results of the slump test for different combinations of ASF and PEA, with the lowest and highest values of 4 5/6 inches for M1 and 3 1/5 inches for M7. According to ACI 211.11 [57], these ranges describe the potential use of the aggregate in construction. Batches M1 to M5 show slack values suitable for columns. On the contrary, combinations M3, M4, M5, and M6 are suitable for reinforced concrete beams and walls, where the level of workability is designed to coincide with the binding strength

in the mixture. Mixture M7, with the lowest slump value, is suitable for surface applications, such as roads and slabs, where the low workability is favorable for cohesive strength and compressive strength.

Table 7. Fresh concrete tests

Identification of mixture	Slump (in)	Temperature (°C)	Unit weight (Kg/m3)	Air content (%)
M1	4 5/6"	27.43	2285.95	1.00
M2	4 1/2"	26.83	2382.90	1.10
M3	4 1/4"	26.78	2367.48	1.20
M4	4 1/8"	25.93	2345.62	1.30
M5	4 1/16"	25.53	2331.52	1.30
M6	3 5/6"	25.03	2326.43	1.40
M7	3 1/5"	24.89	2322.67	1.50

The temperature test enabled us to record the temperature of the fresh concrete. This factor influences the setting, curing, and final strength of the material. The thermometric data showed a decreasing trend, with the highest temperature for M1 at 27.43 °C and the lowest for M7 at 24.89 °C. These thermal discrepancies are likely due to the ambient production conditions and the time gaps between each batch. Keeping the optimal temperature reduces the risk of cracking due to thermal gradients and the problem of evaporation loss during the curing process. This problem is exacerbated during extreme weather conditions in Arequipa, Huancayo, Cajamarca, and Puno. Within these geoclimatic vicinities, thermoregulation of the cementitious matrix constitutes a pivotal determinant of both monolithic tenacity and endurance.

A test by mass was carried out to measure the compactivity, as a proxy for internal cohesion and the associated strength of the fresh mixture. Gradients were evident, with M1 having 2285.95 kg/m³ and M7 having 2322.67 kg/m³. These values are within the accepted range for normal concrete (2200– 2400 kg/m³ or 137–150 lb/ft³) [57], i.e., the ones most commonly used in road and highway construction, building blocks, and trafficable pavements. The results confirm that the specific mass of the mix is appropriate for Peruvian civil construction projects involving high structural load-bearing requirements.

In the denouement, air content was quantified, yielding 1.00% for M1 and 1.50% for M7. This aerometric assay elucidates the volumetric prevalence of gaseous inclusions either as intentional admixtures or inadvertent entrainments during mechanical homogenization. The air retention profile attained during experimentation ostensibly augmented cry-resilience via mitigation of deleterious freeze-thaw cycles, potentially amplifying structural tenacity [58]. In subnivean

geographies like Puno, Cajamarca, and Cusco, where cryogenic thresholds prevail, microporous entrainments act prophylactically against disintegration through exfoliation and fractural propagation. Similarly, in environments with harmful halides, aeric regulation strengthens the resistance of concrete to the aggressive ionic seal penetration.

4.2. Exudation

Figure 6 illustrates the relationship between the percentages of exudation without ASF (aguaje shell fiber) and PEA (shrimp exoskeleton ash) and the different levels of

exudation with ASF and PEA fibers. It can be observed that bleeding became less with the addition of more exudation of ASF and PEA. The highest bleeding without additives (M1) was 0.00081%. In contrast, M7, which contains a higher amount of ASF and PEA, had the least bleeding at 0.00060%. The decrease in bleeding demonstrates that the ASF and PEA additives do assist in the reduction of the concrete surface’s water head, resulting in the mixture’s avoidance of segregation or bleeding. It may improve the internal concrete cohesion, water uniformity during the setting of the mixture, and overall durability of the structure.

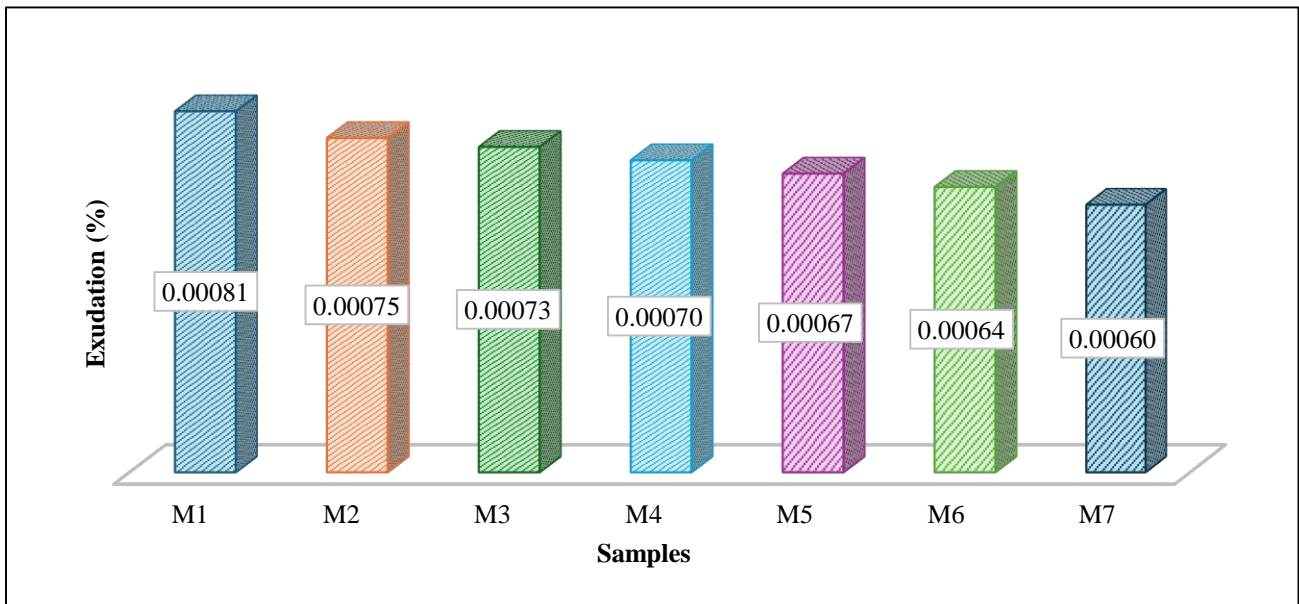


Fig. 6 Exudation

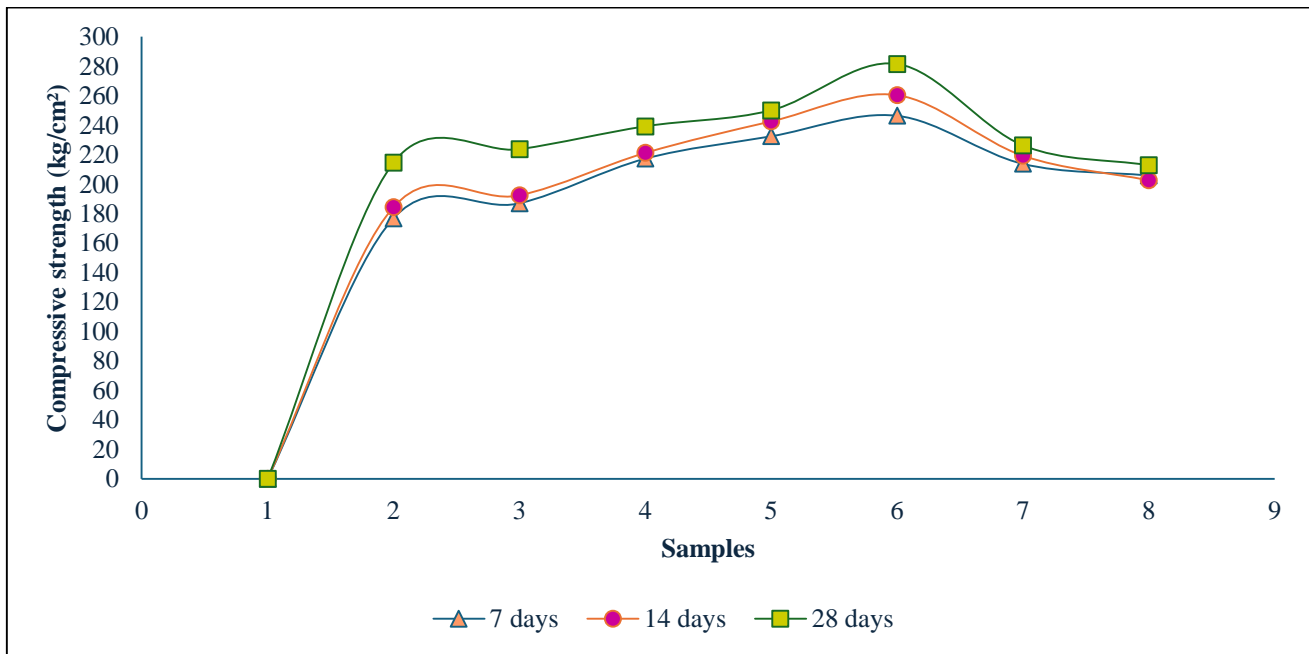


Fig. 7 Compressive strength

4.3. Compressive Strength

Figure 7 contains the results from the compressive strength tests carried out on the concrete samples mixed with Aguaje Shell Fiber (ASF) and Shrimp Exoskeleton Ash (PEA) at 7, 14, and 28 days. The reference sample (M1) without addition reached a 28-day strength of 214.49 kg/cm². At 0.70% ASF and 1.50% PEA (M2), the strength increased to 223.61 kg/cm², 4.25% higher. With 0.90% ASF and 2.00% PEA (M3), the strength was 239.17 kg/cm², which was 11.50% greater. Sample M4, which had 1.10% ASF and 2.50% PEA, achieved a strength of 250.01 kg/cm², which was 16.56% higher than the base sample. Sample M5, containing 1.30% ASF and 1.50% PEA, achieved the highest compressive strength of 281.50 kg/cm², which was 31.24%, the greatest increase. Sample M6 (1.50% ASF + 2.00% PEA) had a compressive strength of 226.31 kg/cm², which was 5.51% higher. Lastly, sample M7 (1.70% ASF + 2.50% PEA) achieved a strength of 212.75 kg/cm², which was 0.81% higher. The results illustrate that sample M5 is the optimized dosage with the highest mechanical performance; excessively high additive content was detrimental to the performance of the concrete.

4.4. Indirect Tensile Strength

Figure 8 shows the results of the indirect tensile strength test on concrete samples with different percentages of Aguaje Shell Fiber (ASF) and Shrimp Exoskeleton Ash (PEA) added. The reference sample (M1), without additives, reached a strength of 22.34 kg/cm² at 28 days. With the incorporation of 0.70% ASF and 1.50% PEA (M2), the strength increased to 23.46 kg/cm², representing an increase of 5.03%. Sample M3 (0.90% ASF + 2.00% PEA) reached 25.89 kg/cm², with an increase of 15.89%, while M4 (1.10% ASF + 2.50% PEA) registered 32.99 kg/cm², representing an increase of 47.67%. Sample M5, with 1.30% ASF and 1.50% PEA, obtained the highest strength with 39.68 kg/cm², showing an increase of 77.60% compared to the sample without addition. In the case of sample M6 (1.50% ASF + 2.00% PEA), the strength was 35.75 kg/cm², equivalent to an increase of 60.03%. Finally, sample M7 (1.70% ASF + 2.50% PEA) achieved a strength of 30.41 kg/cm², with an increase of 36.12%. These results suggest that the combined addition of ASF and PEA significantly improves the tensile strength of concrete, with the M5 dosage being the most efficient; however, higher percentages could lead to a progressive decrease in performance.

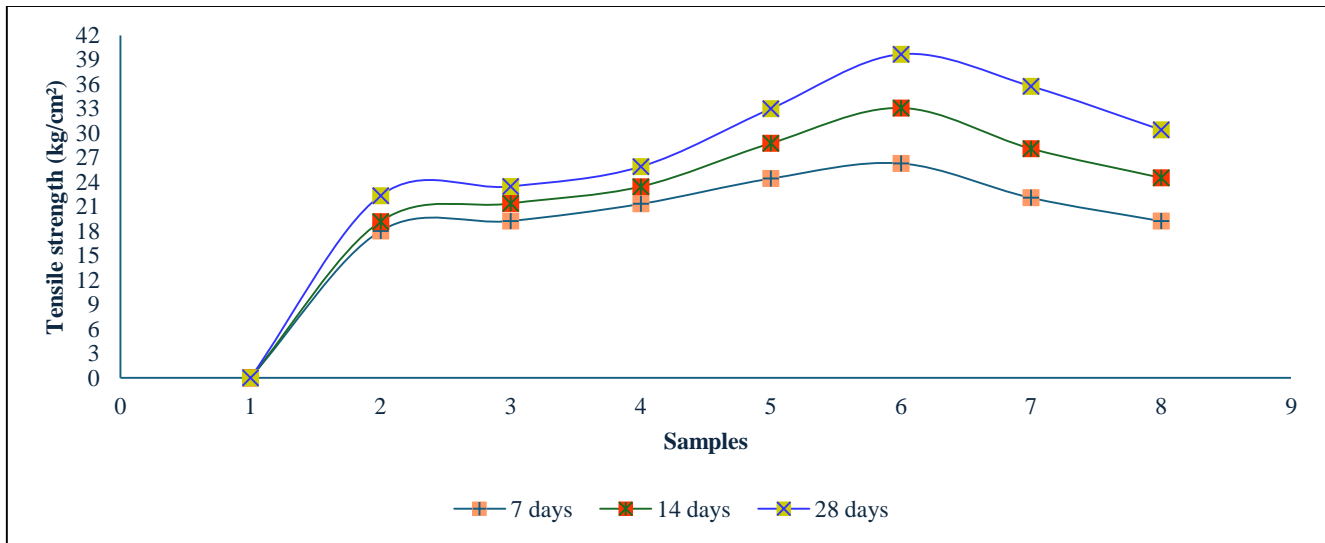


Fig. 8 Tensile strength

4.5. Flexural Strength

Figure 9 shows the results of the flexural strength test of the concrete samples at 28 days, evaluating the effect of adding Aguaje Shell Fiber (ASF) and Shrimp Exoskeleton Ash (PEA). The reference sample (M1), without additives, obtained a strength of 41.13 kg/cm². When 0.70% ASF and 1.50% PEA (M2) were added, the strength increased to 45.95 kg/cm², i.e., an increase of 11.71%. Sample M3 (0.90% ASF + 2.00% PEA) recorded 56.84 kg/cm² (+38.19%), while M4 (1.10% ASF + 2.50% PEA) reached 66.44 kg/cm², representing an increase of 61.54%. The highest strength was obtained by sample M5 (1.30% ASF + 1.50% PEA), with

79.75 kg/cm², representing an increase of 93.89% compared to M1. In the case of M6 (1.50% ASF + 2.00% PEA), 60.68 kg/cm² (+47.52%) was achieved, and finally M7 (1.70% ASF + 2.50% PEA) showed a slight decrease compared to the previous ones, reaching 56.85 kg/cm² (+38.23%). These results indicate that the combination of ASF and PEA significantly improves the flexural strength of concrete, with the M5 dosage being the most favorable; however, as in other tests, an excess of additives can compromise mechanical performance.

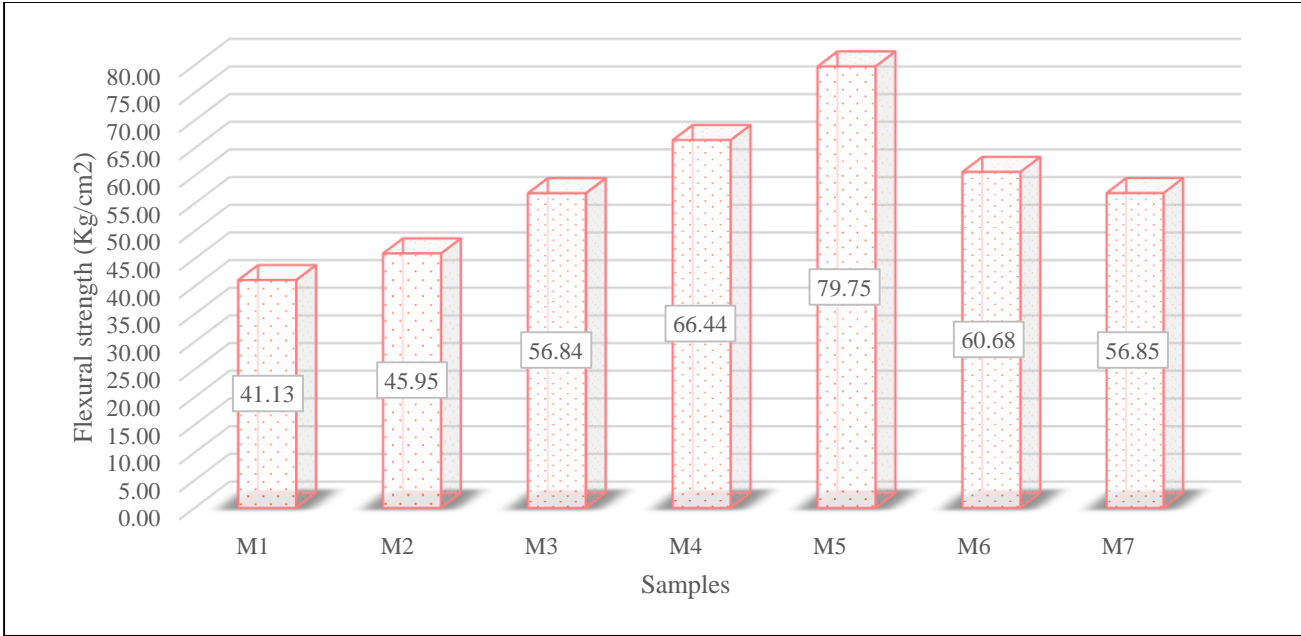


Fig. 9 Flexural strength

4.6. Compressive Strength with Sulfates

Figure 10 shows the sulfate compressive strength test (kg/cm²) of the different mixtures with additions of Aguaje Shell Fiber (ASF) and Shrimp Exoskeleton Ash (PEA) after 50 days of curing. The results show that the mixture without additives (M1) had a strength of 218.45 kg/cm², while the mixtures with ASF and PEA additives showed a progressive increase in strength. Mixture M2, with 0.70% ASF and 1.50% PEA, reached a strength of 219.34 kg/cm², which represented a small increase over the mixture without additives. As the dosage of ASF and PEA increased, a more significant increase

in compressive strength was observed, with mixture M5, with 1.30% ASF and 1.50% PEA, reaching a strength of 234.31 kg/cm², the highest of all mixtures. Although the mixtures with higher proportions of ASF and PEA, such as M6 and M7, showed a slight decrease in strength compared to M5, the results remain competitive, reaching 229.98 kg/cm² and 227.98 kg/cm², respectively. These results indicate that the addition of ASF and PEA improves the resistance of concrete to sulfate attack, although with variations depending on the dosages.

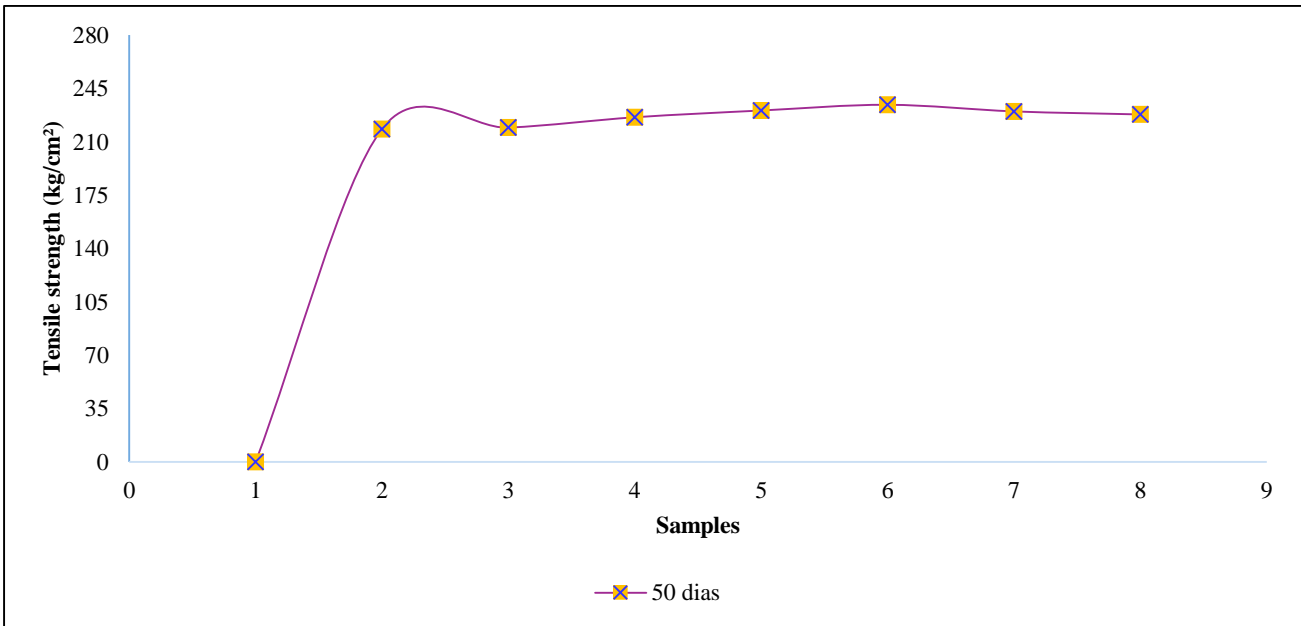


Fig. 10 Compressive strength with sulfates

4.7. Statistical Evaluation of the Mechanical Behavior of Concrete

An examination of the coefficients of variation presented in Table 8 shows that the experimental results exhibit a controlled level of dispersion across all tests, indicating consistent behaviour among the specimens within each mixture.

For compressive strength, the coefficients of variation range from 0.64% to 3.75%, reflecting a very low level of variability between the tested specimens. These values indicate excellent repeatability of the test and confirm that the reported average compressive strengths are highly representative of the actual behaviour of the concrete.

In the case of indirect tensile strength, the coefficients of variation fall within a range of approximately 10.39% to 16.20%. Although these values are higher than those observed for compressive strength, this behaviour is expected due to the greater sensitivity of tensile tests to internal defects and microcracking. Nevertheless, the observed variability remains

within acceptable limits and does not suggest experimental inconsistencies.

For flexural strength, the coefficients of variation vary between 3.39% and 7.10%, indicating a relatively uniform mechanical response of the concrete under flexural loading. These values suggest that the test was well controlled and that the flexural strength results can be considered reliable.

Finally, the coefficients of variation associated with sulphate resistance remain low, ranging from 2.26% to 2.61%, which demonstrates a high level of consistency in the durability test results. This low dispersion confirms the reliability of the sulphate resistance measurements.

Overall, the coefficients of variation obtained indicate that the experimental data show limited dispersion and fall within acceptable ranges for concrete testing, supporting the reliability of the reported average values and the validity of the conclusions drawn from the study.

Table 8. Statistical summary of mechanical and durability properties of concrete

Sample	Compression 28 days (kg/cm ²)	CV (%)	Tension 28 days	CV (%)	Bending 28 days	CV (%)	Sulphates 50 days	CV (%)
M1	214.49 ± 8.03	3.75	22.34 ± 3.09	13.82	41.13 ± 1.92	4.66	218.45 ± 5.25	2.40
M2	223.61 ± 3.30	1.48	23.46 ± 3.55	15.11	45.95 ± 2.38	5.19	219.34 ± 5.73	2.61
M3	239.17 ± 6.48	2.71	25.89 ± 4.20	16.2	56.84 ± 2.31	4.07	226.13 ± 5.86	2.59
M4	250.01 ± 4.97	1.99	32.99 ± 4.61	13.96	66.44 ± 3.00	4.51	230.57 ± 5.22	2.26
M5	281.50 ± 1.80	0.64	39.68 ± 4.12	10.39	79.75 ± 2.71	3.39	234.31 ± 5.59	2.38
M6	226.31 ± 6.50	2.87	35.75 ± 4.69	13.11	60.68 ± 4.31	7.1	229.98 ± 5.70	2.48
M7	212.75 ± 7.53	3.54	30.41 ± 4.42	14.52	56.85 ± 3.29	5.79	227.98 ± 5.78	2.54

5. Discussions

Considering the few studies focusing on the integration of Aguaje Shell Fibre (ASF) and Shrimp Exoskeleton Ash (PEA) in concrete, the current findings must be contextualized with other natural fibres and bio-based ashes, including the explanations for the observed mechanical and durability behaviour. Previous research consistently shows that natural fibers can improve concrete’s compressive strength when dosages are properly managed. Ranjitham et al. noted that adding coconut fiber increased compressive strength, with the best result at 3% fiber content, achieving,

19.5 N/mm², followed by 2% (18.1 N/mm²) and 1% (18.0 N/mm²) [59]. Mydin et al. similarly noted that Agave fiber improved compressive strength of concrete under controlled conditions, increasing compressive strength from 1.75 MPa to 2.97 MPa after 28 days of curing [27]. Also, Chellapandian et al. showed that 2% of flax fiber content led to a significant increase in compressive strength [60]. These findings align with this present study, where, of the examined mixtures, the combination of 1.30% ASF and 1.50% PEA resulted in the highest compressive strength (281.50 kg/cm²) at 28 days,

representing a significant increase compared to the control mixture (214.49 kg/cm²).

The findings suggest that the addition of ash and fibre to a certain point does yield performance gains; however, any further increases do not result in such gains. The compressive strength reduction in mixtures M6 and M7 is due to insufficiently homogeneous dispersion of the cementitious matrix and fibre. Insufficiently homogeneously dispersed fibres create zones of weakness by increasing fibre-fibre contacts, which in turn result in balling effects and fluidity fails to allow settlement. Moreover, when there is an excessive amount of short, natural fibres, a definitive length of which horizontally spans the cement matrix, their ability to intercept and transfer stress is indirectly diminished, which is consistent with much of the literature that discusses fibre-reinforced concretes.

The trend is rather consistent with regard to flexural strength behavior. Sabarish recorded flexural strength values of 5.72, 5.88, and 6.56 N/mm² at 7, 14, and 28 days of curing, respectively. These values are also significantly higher than

the respective control values of 4.36 N/mm² at 7 days, 5.06 N/mm² at 14 days, and 5.12 N/mm² at 28 days [61]. In this study, the mixture with 1.30% ASF and 1.50% PEA showed the greatest increase in flexural strength (about 93.89%) when compared to the control. The decline of the crack-bridging mechanism explains the aguaje fibres that delay crack accumulation and improve the load transfer after cracking. In contrast, most of the composite flexural performance obtained was lower due to the higher levels of fibres, confirming that the clustering of fibres and poor orientational placement prevent adequate redistribution of the stress.

The results for the tensile strength justified the importance of ASF on reinforcement. Da Costa Santos and Archbold noted that using flax and hemp fibres, tensile strength was improved by about 101% with little effect on the elastic modulus [62]. They also noted these materials could enable circular economies in construction and other frameworks in the most optimally efficient ways. A tensile strength increase of about 77.60% was noted in this study for the most optimal ASF-PEA ratio within the range, and it is also believed to be due to the fibre matrix interaction within the Interfacial Transition Zone (ITZ), where the fibres act as micro reinforcements bridging tensile gaps and relieving stress concentrations.

From a microstructural and chemical perspective, the part shrimp exoskeleton ash plays in the chemical interactions is positive. PEA has a high calcium carbonate (CaCO₃) content, which acts as a filler and nucleating agent within the cement matrix. When mixed with cement, finely ground CaCO₃ enhances hydration by providing nucleation sites for the formation of calcium silicate hydrate (C-S-H), which creates a denser microstructure and refined pore structure. The ITZ (Interfacial Transition Zone) is denser, enhancing the quality and reducing the porosity around the aggregates and fibres, increasing the microstructure's and the full composite's mechanical performance and durability. The contribution of PEA helps to densify the matrix and refine the interfacial transition zone; although PEA does not exhibit true pozzolanic activity, its interaction with the fiber reinforcement provided by ASF generates a beneficial synergistic effect on the mechanical performance of the composite.

The noted reduction in bleeding and settlement of the fresh concrete mixtures supports this interpretation. Islam and Ahmed noted that jute fibres, in composite materials, prevented the settlement of materials, more so with 10 mm fibres than with 20 mm fibres [63]. The current study noted a reduction in bleeding with increased ASF (alkali-silica fibres) and PEA, which indicates increased stability of the paste and the interaction of the fibres with the paste; however, the presence of excessive fibres can negatively affect the workability and consistency.

Concerning ASF and PEA mixtures, improvements in the resistance to sulphate attacks are in line with Shahzeb et al.'s findings, where they documented positive results on concrete exposed to sulphates with the inclusion of 20% banana leaf ash [64]. Here, the 7% increase in sulfate resistance of the best concrete mix can be linked to the densified matrix, the lower permeability, and the better quality of the ITZ, which, combined, restrict the ingress of sulfate and the subsequent deterioration mechanisms. Moreover, the observed sulfate resistance at higher dosages, where an even greater resistance was expected, indicates the criticality of proportioning to avert the negative effects of fibre agglomeration due to paste deficiency.

The cementitious matrix structure helps to explain the mechanical enhancements and the improvement of durability in the ASF-PEA hybrid concrete. Aguaje shell fibres assist in the microcrack bridging and microcrack formation control, leading to the redistribution of stress and internal damage. This is reflected in the indirect increases of compressive strength and increases in flexural and indirect tensile strengths. Cartilaginous shrimp exoskeleton ash, which contains calcium carbonate (CaCO₃), positively alters the microstructure via the fill and nucleation effects, which leads to compactness in the matrix and improved quality of the Interfacial Transition Zone (ITZ) between the paste and aggregates and fibres. The combined action of these mechanisms contributes towards the internal deterioration under the influence of expansive products, progressive microcracking, and increased compressive strength retention in ASF-PEA hybrid concrete. This also helps to explain the optimal hybrid dosage.

6. Conclusion

The findings of this research demonstrate that the amalgamation of Aguaje Shell Fibre (ASF) and Shrimp Exoskeleton Ash (PEA) is beneficial to concrete in both fresh and hardened states, as long as the dosages are kept in the right amounts. In the fresh state, this hybrid combination has been documented to decrease bleeding by 26% and increase the amount of entrapped air, which leads to improved cohesion and compaction of the concrete, resulting in a denser and more stable concrete matrix.

From a performance and mechanical perspective, the concrete performance improved as the ASF content increased to a point where the optimal dosage was 1.30% combined with 1.50% PEA. At this ratio, the increased compressive strength at 28 days was 31.24%. In the same light, and in comparison to the reference concrete, the performance was vastly improved as there was an increase of 77.60% and 93.89% in tensile and flexural strengths, respectively. It is also pertinent to state that a decrease in performance was witnessed in the

ASF content when it increased beyond the optimal dosage. It, therefore, suggests that a sufficient balance of ASF and PEA is critical.

Given that the developed concrete attained a compressive strength a bit above the characteristic value of ($f'c=210$ kg/cm²), the ASF-PEA hybrid concrete can be deemed appropriate for standard construction practices. This encompasses low to mid-rise structures: for the structural components (columns, beams, slabs), and for lightweight urban infrastructure, including low to mid traffic urban pavement, sidewalks, drainage (the channel type), and non-structural precast drainage. This set of uses corresponds to the strength attained and the performance of the concrete in both the fresh and the hardened states.

Regarding durability, ASF and PEA together helped create concrete that is less susceptible to mechanical deterioration due to sulphate attack. This is evidenced by the compressive strength after sulphate exposure, which shows an increase of about 7% in comparison to the reference concrete,

indicating it behaved satisfactorily in a severe sulphate environment.

These outcomes should, however, be viewed with caution. The experimental programme was carried out in a laboratory environment, and the durability assessment was limited to one type of sulphate attack and did not include other aggressive agents, such as chlorides, or other processes like drying shrinkage. As such, the future assessment of ASF-PEA concrete should be directed towards performance evaluations under actual service conditions, including sustained and dual exposure to a variety of environmental and mechanical influences.

Furthermore, additional microstructural studies, Life Cycle Assessment (LCA), and mix design optimisations would help in advancing our understanding of the hybrid concrete's potential as a sustainable construction material from both a technical and environmental performance perspective.

References

- [1] Marine Valesan, Beatriz Fedrizzi, and Miguel Aloysio Sattler, "Advantages and Disadvantages of using Green Skin in Residential Buildings in Porto Alegre According to its Residents," *Ambiente Construído*, vol. 10, no. 3, pp. 55-67, 2010. [[CrossRef](#)] [[Google Scholar](#)] [[Publisher Link](#)]
- [2] Mahmure Övül Arıoğlu Akan, Dileep G. Dhavale, and Joseph Sarkis, "Greenhouse Gas Emissions in the Construction Industry: An Analysis and Evaluation of a Concrete Supply Chain," *Journal of Cleaner Production*, vol. 167, pp. 1195-1207, 2017. [[CrossRef](#)] [[Google Scholar](#)] [[Publisher Link](#)]
- [3] Clinker Replacement: A Key Trend in the Cement Industry, Proquicesa, 2024. [Online]. Available: <https://www.proquicesa.com/sustitucion-clinker-en-la-industria-del-cemento/>
- [4] Ready-Mix Concrete (RM) Statistics, DANE, 2025. [Online]. Available: <https://www.dane.gov.co/index.php/estadisticas-por-tema/construccion/estadisticas-de-concreto-premezclado>
- [5] G. Habert et al., "Environmental Impacts and Decarbonization Strategies in the Cement and Concrete Industries," *Nature Reviews Earth and Environment*, vol. 1, no. 11, pp. 559-573, 2020. [[CrossRef](#)] [[Google Scholar](#)] [[Publisher Link](#)]
- [6] Freek Paul Bos et al., "The Realities of Additively Manufactured Concrete Structures in Practice," *Cement and Concrete Research*, vol. 156, pp. 1-14, 2022. [[CrossRef](#)] [[Google Scholar](#)] [[Publisher Link](#)]
- [7] Sector Report: Aquaculture Performance of Aquaculture Activity, Sector Report, Ministry of Production, 2024. [Online]. Available: https://www.producepresarial.pe/wp-content/uploads/2024/04/9-PPT-Sector-Acuicultura-Febrero-2024_rev-1.pdf
- [8] Natalija Topić Popović et al., "Shell Waste Management and Utilization: Mitigating Organic Pollution and Enhancing Sustainability," *Applied Sciences*, vol. 13, no. 1, pp. 1-18, 2023. [[CrossRef](#)] [[Google Scholar](#)] [[Publisher Link](#)]
- [9] Bulletin, Utilization of Mauritia Flexuosa Waste, Productive Innovation and Technology Transfer Center Maynas, Gob.pe, 2024. [Online]. Available: <https://www.gob.pe/institucion/citeproductivo-maynas/informes-publicaciones/5514803-aprovechamiento-de-los-residuos-de-mauritia-flexuosa>
- [10] National Service of Natural Areas Protected by the State: Cordillera Azul National Park, Gob.pe, 2019. [Online]. Available: <https://www.gob.pe/institucion/sernanp/informes-publicaciones/1948130-parque-nacional-cordillera-azul>
- [11] The Aguaje Fruit: A Fruit with History and Commercial Potential, SPDA Actualidad Ambiental, 2024. [Online]. Available: <https://www.actualidadambiental.pe/el-aguaje-un-fruto-con-historia-y-potencial-comercial/>
- [12] M.C. Arimanwa, P.C. Anyadiegwu, and N.P. Ogbonna, "The Potential Use of Coconut Fibre Ash (CFA) in Concrete," *The International Journal of Engineering and Science (IJES)*, vol. 9, no. 1, pp. 68-75, 2020. [[Google Scholar](#)]
- [13] Constance Tunje, Richard Onchiri, and Joseph Thuo, "Concrete Microstructure Study on the Effect of Sisal Fiber Addition on Sugarcane Bagasse Ash Concrete," *The Open Civil Engineering Journal*, vol. 15, no. 1, pp. 320-329, 2021. [[CrossRef](#)] [[Google Scholar](#)] [[Publisher Link](#)]

- [14] Patrick Aaniamenga Bowan, "Cocoa Pod Husk Ash as Partial Replacement of Cement in Concrete Production," *Communications in Applied Sciences*, vol. 10, pp. 1-14, 2022. [[Google Scholar](#)] [[Publisher Link](#)]
- [15] S. Govindhan, and S. Thamizha, "Experimental Study of Concrete using Seashell and Flyash," *International Research Journal of Engineering and Technology (IRJET)*, vol. 6, no. 3, pp. 403-411, 2019. [[Google Scholar](#)] [[Publisher Link](#)]
- [16] Sri Vinay Chowdari Dasari, A. Deiveegan, and N.R.M. Reddy, "Strength Characteristics of Crab Shell Powder and Silica Fume based Concrete - A Comparison of M35 and M70 Grade Concrete," *NeuroQuantology*, vol. 20, no. 16, pp. 2237-2254, 2022. [[CrossRef](#)] [[Publisher Link](#)]
- [17] Yi Han, Runsheng Lin, and Xiao-Yong Wang, "Performance of Sustainable Concrete Made from Waste Oyster Shell Powder and Blast Furnace Slag," *Journal of Building Engineering*, vol. 47, 2022. [[CrossRef](#)] [[Google Scholar](#)] [[Publisher Link](#)]
- [18] Krystel Clarissa Rojas Mego et al., "Arbuscular Mycorrhizal Fungi Associated with Capirona (*Calycophyllum Spruceanum* Benth.) in the Peruvian Amazon," *Folia Amazónica*, vol. 33, no. 2, pp. 1-13, 2024. [[CrossRef](#)] [[Google Scholar](#)] [[Publisher Link](#)]
- [19] Carlos Victor Lamarão, *Amazon Fruits: Biodiversity, Regionalism and Artisanal and Industrial By-Products Under Fermentation Processes*, 1st ed., Fermented Foods of Latin America, CRC Press, pp. 185-201, 2017. [[Google Scholar](#)] [[Publisher Link](#)]
- [20] Silvia Virginia Melgarejo Cabello et al., "Effect of Particle Size and Temperature on Aguaje (*Mauritia Flexuosa*) Peel Flour and Application in Cookies," *LA Referencia, Revistas - Universidad Nacional Agraria La Molina*, 2023. [[Google Scholar](#)] [[Publisher Link](#)]
- [21] R.N. Cavalcanti et al., *Uses and Applications of Extracts from Natural Sources*, 2nd ed., Green Chemistry Series, Royal Society of Chemistry, pp. 1-65, 2022. [[CrossRef](#)] [[Google Scholar](#)] [[Publisher Link](#)]
- [22] Rafael Fernández de Alaiza García Madrigal et al., "Use of Native and Non-Native Shrimp (Penaeidae, Dendrobranchiata) in World Shrimp Farming," *Reviews in Aquaculture*, vol. 10, no. 4, pp. 899-912, 2018. [[CrossRef](#)] [[Google Scholar](#)] [[Publisher Link](#)]
- [23] Nur Izyan Wan Azelee et al., "Sustainable Valorization Approaches on Crustacean Wastes for the Extraction of Chitin, Bioactive Compounds and their Applications-A Review," *International Journal of Biological Macromolecules*, vol. 253, 2023. [[CrossRef](#)] [[Google Scholar](#)] [[Publisher Link](#)]
- [24] Farnaz Assa et al., "Chitosan Magnetic Nanoparticles for Drug Delivery Systems," *Critical Reviews in Biotechnology*, vol. 37, no. 4, pp. 492-509, 2017. [[CrossRef](#)] [[Google Scholar](#)] [[Publisher Link](#)]
- [25] Moutoshi Chakraborty et al., "Mechanism of Plant Growth Promotion and Disease Suppression by Chitosan Biopolymer," *Agriculture*, vol. 10, no. 12, pp. 1-30, 2020. [[CrossRef](#)] [[Google Scholar](#)] [[Publisher Link](#)]
- [26] Bahareh Azimi et al., "Electrosprayed Shrimp and Mushroom Nanochitins on Cellulose Tissue for Skin Contact Application," *Molecules*, vol. 26, no. 14, pp. 1-15, 2021. [[CrossRef](#)] [[Google Scholar](#)] [[Publisher Link](#)]
- [27] M.A.O. Mydin et al., "Optimization of Mechanical Properties of Raw Agave Fibre-Reinforced Lightweight Foamed Concrete," *Archives of Metallurgy and Materials*, vol. 69, no. 2, pp. 753-759, 2024. [[CrossRef](#)] [[Google Scholar](#)] [[Publisher Link](#)]
- [28] Emilio Vélez et al., "Coconut-Fiber Composite Concrete: Assessment of Mechanical Performance and Environmental Benefits," *Fibers*, vol. 10, no. 11, pp. 1-12, 2022. [[CrossRef](#)] [[Google Scholar](#)] [[Publisher Link](#)]
- [29] R. Sathia, and Ramalingam Vijayalakshmi, "Fresh and Mechanical Property of Caryota-Urens Fiber Reinforced Flowable Concrete," *Journal of Materials Research and Technology*, vol. 15, pp. 3647-3662, 2021. [[CrossRef](#)] [[Google Scholar](#)] [[Publisher Link](#)]
- [30] Rayed Alyousef et al., "Effect of Sheep Wool Fiber on Fresh and Hardened Properties of Fiber Reinforced Concrete," *International Journal of Civil Engineering and Technology (IJCIET)*, vol. 10, no. 5, pp. 190-199, 2019. [[Google Scholar](#)] [[Publisher Link](#)]
- [31] S. Tiwari, A.K. Sahu, and R.P. Pathak, "Mechanical Properties and Durability Study of Jute Fiber Reinforced Concrete," *IOP Conference Series: Materials Science and Engineering, International Conference on Advanced Materials Behavior & Characterization (ICAMBC_2020)*, Chennai, India, vol. 961, no. 1, pp. 1-13, 2020. [[CrossRef](#)] [[Google Scholar](#)] [[Publisher Link](#)]
- [32] Solomon Asrat Endale et al., "Rice Husk Ash in Concrete," *Sustainability*, vol. 15, no. 1, pp. 1-26, 2023. [[CrossRef](#)] [[Google Scholar](#)] [[Publisher Link](#)]
- [33] Sanskar Soni, and Devesh Ojha, "A Study on Use of Rice Husk Ash in Concrete," *Journal of Mechanical and Construction Engineering (JMCE)*, vol. 1, no. 1, pp. 1-4, 2021. [[CrossRef](#)] [[Google Scholar](#)] [[Publisher Link](#)]
- [34] Ayesha Siddika, Md. Abdullah Al Mamun, and Md. Hedayet Ali, "Study on Concrete with Rice Husk Ash," *Innovative Infrastructure Solutions*, vol. 3, no. 1, pp. 1-9, 2018. [[CrossRef](#)] [[Google Scholar](#)] [[Publisher Link](#)]
- [35] Jawad Ahmad et al., "Concrete Made with Partially Substitution Corn Cob Ash: A Review," *Case Studies in Construction Materials*, vol. 18, pp. 1-18, 2023. [[CrossRef](#)] [[Google Scholar](#)] [[Publisher Link](#)]
- [36] P. Murthi, K. Poongodi, and R. Gobinath, "Effects of Corn Cob Ash as Mineral Admixture on Mechanical and Durability Properties of Concrete - A Review," *IOP Conference Series: Materials Science and Engineering, Sustainable Construction Technologies & Advancements in Civil Engineering (ScTACE-2020)*, Bhimavaram, India, vol. 1006, no. 1, pp. 1-13, 2020. [[CrossRef](#)] [[Google Scholar](#)] [[Publisher Link](#)]
- [37] Jennef Carlos Tavares et al., "Use of Banana Leaf Ash as Partial Replacement of Portland Cement in Eco-Friendly Concretes," *Construction and Building Materials*, vol. 346, 2022. [[CrossRef](#)] [[Google Scholar](#)] [[Publisher Link](#)]

- [38] Ibrahim Saad Agwa et al., “Effects of using Rice Straw and Cotton Stalk Ashes on the Properties of Lightweight Self-Compacting Concrete,” *Construction and Building Materials*, vol. 235, pp. 1-12, 2020. [[CrossRef](#)] [[Google Scholar](#)] [[Publisher Link](#)]
- [39] Gashaw Abebaw, Bahiru Bewket, and Shumet Getahun, “Experimental Investigation on Effect of Partial Replacement of Cement with Bamboo Leaf Ash on Concrete Property,” *Advances in Civil Engineering*, vol. 2021, no. 1, pp. 1-9, 2021. [[CrossRef](#)] [[Google Scholar](#)] [[Publisher Link](#)]
- [40] David Obinna Nduka et al., “Mechanical and Durability Property Dimensions of Sustainable Bamboo Leaf Ash in High-Performance Concrete,” *Clean Engineering and Technology*, vol. 11, pp. 1-13, 2022. [[CrossRef](#)] [[Google Scholar](#)] [[Publisher Link](#)]
- [41] Ma. Bernadeth B. Lim et al., “Pulverized Blue Swimming Crab Shell Utilized as Partial Replacement for Sand in Concrete Mixture,” *The Palawan Scientist*, vol. 13, no. 1, pp. 31-43, 2021. [[Google Scholar](#)] [[Publisher Link](#)]
- [42] Tuhua Zhong et al., “Interfacial Interactions and Reinforcing Mechanisms of Cellulose and Chitin Nanomaterials and Starch Derivatives for Cement and Concrete Strength and Durability Enhancement: A Review,” *Nanotechnology Reviews*, vol. 11, no. 1, pp. 2673-2713, 2022. [[CrossRef](#)] [[Google Scholar](#)] [[Publisher Link](#)]
- [43] Gideon Olukunle Bamigboye et al., “The Use of Senilia Senilis Seashells as a Substitute for Coarse Aggregate in Eco-Friendly Concrete,” *Journal of Building Engineering*, vol. 32, pp. 1-12, 2020. [[CrossRef](#)] [[Google Scholar](#)] [[Publisher Link](#)]
- [44] Chioma Emmanuella Njoku et al., “Utilization of Quarry Dust and Periwinkle Shell ash in Concrete Production,” *Environmental Science and Pollution Research*, vol. 32, no. 54, pp. 29957-29966, 2025. [[CrossRef](#)] [[Google Scholar](#)] [[Publisher Link](#)]
- [45] Ahmed Mustafa Maglad et al., “Assessing the Mechanical, Durability, Thermal and Microstructural Properties of Sea Shell ash based Lightweight Foamed Concrete,” *Construction and Building Materials*, vol. 402, 2023. [[CrossRef](#)] [[Google Scholar](#)] [[Publisher Link](#)]
- [46] Natt Makul, *Principles of Cement and Concrete Composites*, 1st ed., Springer Cham, 2021. [[CrossRef](#)] [[Google Scholar](#)] [[Publisher Link](#)]
- [47] Joseph O. Ukpata et al., “Effects of Aggregate Sizes on the Performance of Laterized Concrete,” *Scientific Reports*, vol. 14, no. 1, pp. 1-20, 2024. [[CrossRef](#)] [[Google Scholar](#)] [[Publisher Link](#)]
- [48] Ignatius Chigozie Onyechere et al., “An Investigation on the Compressive Strength of Concrete Made from Three Different Coarse Aggregates,” *International Research Journal of Modernization in Engineering Technology and Science*, vol. 3, no. 2, pp. 281-289, 2021. [[Google Scholar](#)] [[Publisher Link](#)]
- [49] Tatiana Jaramillo-Vivanco et al., “Three Amazonian Palms as Underestimated and Little-Known Sources of Nutrients, Bioactive Compounds and Edible Insects,” *Food Chemistry*, vol. 372, pp. 1-13, 2022. [[CrossRef](#)] [[Google Scholar](#)] [[Publisher Link](#)]
- [50] Majda Sfiligoj Smole et al., *Non-Conventional Cellulose Fibres*, Surface Properties of Non-Conventional Cellulose Fibres, Springer, Cham, pp. 17-48, 2019. [[CrossRef](#)] [[Google Scholar](#)] [[Publisher Link](#)]
- [51] N. Suryawanshi, S.E. Jujjavarapu, and S. Ayothiraman, “Marine Shell Industrial Wastes - An Abundant Source of Chitin and its Derivatives: Constituents, Pretreatment, Fermentation, and Pleiotropic Applications - A Revisit,” *International Journal of Environmental Science and Technology*, vol. 16, no. 7, pp. 3877-3898, 2019. [[CrossRef](#)] [[Google Scholar](#)] [[Publisher Link](#)]
- [52] Pankaj Bhatt et al., “Developments and Application of Chitosan-based Adsorbents for Wastewater Treatments,” *Environmental Research*, vol. 226, pp. 1-18, 2023. [[CrossRef](#)] [[Google Scholar](#)] [[Publisher Link](#)]
- [53] Oluwashina Philips Gbenedor et al., “Role of CaCO₃ in the Physicochemical Properties of Crustacean-Sourced Structural Polysaccharides,” *Materials Chemistry and Physics*, vol. 184, pp. 203-209, 2016. [[CrossRef](#)] [[Google Scholar](#)] [[Publisher Link](#)]
- [54] Ipei Maruyama et al., “A New Concept of Calcium Carbonate Concrete using Demolished Concrete and CO₂,” *Journal of Advanced Concrete Technology*, vol. 19, no. 10, pp. 1052-1060, 2021. [[CrossRef](#)] [[Google Scholar](#)] [[Publisher Link](#)]
- [55] Md Azree Othuman Mydin et al., “Use of Calcium Carbonate Nanoparticles in Production of Nano-Engineered Foamed Concrete,” *Journal of Materials Research and Technology*, vol. 26, pp. 4405-4422, 2023. [[CrossRef](#)] [[Google Scholar](#)] [[Publisher Link](#)]
- [56] Poliana Bellei et al., “Potential Use of Oyster Shell Waste in the Composition of Construction Composites: A Review,” *Buildings*, vol. 13, no. 6, pp. 1-31, 2023. [[CrossRef](#)] [[Google Scholar](#)] [[Publisher Link](#)]
- [57] ACI PRC-211.1-91, “Standard Practice for Selecting Proportions for Normal, Heavyweight, and Mass Concrete,” American Concrete Institute Standard, pp. 1-38, 1996. [[Google Scholar](#)] [[Publisher Link](#)]
- [58] Beatriz Paola Suri Paredez et al., “Influence of Cocoa Cob Fibre on the Durability and Performance of High-Strength Concrete,” *Civil Engineering and Architecture*, vol. 13, no. 3, pp. 1807-1819, 2025. [[CrossRef](#)] [[Publisher Link](#)]
- [59] M. Ranjitham et al., “Strength Properties of Coconut Fibre Reinforced Concrete,” *AIP Conference Proceedings: International Conference on Materials, Manufacturing and Machining 2019*, Tamilnadu, India, vol. 2128, no. 1, 2019. [[CrossRef](#)] [[Google Scholar](#)] [[Publisher Link](#)]
- [60] Maheswaran Chellapandian, Jeyaprakash Maheswaran, and Nakarajan Arunachelam, “Thermal and Mechanical Properties of a Sustainable Bio-Flax Fibre-based Lightweight Aggregate Concrete,” *Magazine of Concrete Research*, vol. 76, no. 7, pp. 350-365, 2024. [[CrossRef](#)] [[Google Scholar](#)] [[Publisher Link](#)]
- [61] K.V. Sabarish et al., “Strength and Durability Evaluation of Sisal Fibre Reinforced Concrete,” *International Journal of Civil Engineering and Technology (IJCIET)*, vol. 8, no. 9, pp. 741-748, 2017. [[Google Scholar](#)] [[Publisher Link](#)]

- [62] Ana Caroline da Costa Santos, and Paul Archbold, "Suitability of Surface-Treated Flax and Hemp Fibers for Concrete Reinforcement," *Fibers*, vol. 10, no. 11, pp. 1-25, 2022. [[CrossRef](#)] [[Google Scholar](#)] [[Publisher Link](#)]
- [63] Mohammad S. Islam, and Syed JU Ahmed, "Influence of Jute Fiber on Concrete Properties," *Construction and Building Materials*, vol. 189, pp. 768-776, 2018. [[CrossRef](#)] [[Google Scholar](#)] [[Publisher Link](#)]
- [64] Shahzeb Bhutto et al., "Effect of Banana Tree Leaves Ash as Cementitious Material on the Durability of Concrete Against Sulphate and Acid Attacks," *Heliyon*, vol. 10, no. 7, pp. 1-17, 2024. [[CrossRef](#)] [[Google Scholar](#)] [[Publisher Link](#)]